A Surface Defect Detection Method for Cold-rolled Strip Steel Based on Improved YOLOv8

Xiaoning Bo[1,2], Jin Wang[1], Yongqiang Zhao[1]*

[1] School of Electronic Engineering, Taiyuan Institute of Technology, China
[2] School of Information and Communication Engineering, North University of China, China
boxn@tit.edu.cn, wangj@tit.edu.cn, zhaoyongqiang@tit.edu.cn

Abstract

Cold-rolled strip steel has excellent mechanical properties, and it is widely used in the fields such as automotive manufacturing, construction industry, aircraft manufacturing and electronic product manufacturing. However, many different processing defects occur in the manufacturing process of cold-rolled strip steel, and this article proposes a visual detection method based on YOLOv8 to identify the surface defects on cold-rolled strip steel more accurately. Firstly, several common types of defects in cold-rolled strip steel were analyzed. Then, in order to enrich the dataset for subsequent detection, wavelet transform was used for filtering, denoising, and canny edge detection in the image processing stage for obtaining the clearer input model image with the more prominent graphics. Lastly, the CA attention mechanism was added into the YOLOv8 which is useful to improve the features recognition ability of the model, at the same time, the original standard convolution was replaced by DCS convolution and the loss function was optimized which is useful to get the lightweight models. The improved YOLOv8 model was validated on the NEU-DET dataset, the overall detection performance of the model such as the recall, the accuracy, and the average precision has significantly improved.

Keywords: YOLOv8, The CA attention mechanism, DCS convolution, Wavelet denoising

1 Introduction

As a steel product processed by cold rolling processing technology, strip steel generally includes hard alloy steel strips, stainless steel strips, low-carbon steel strips, etc. and it is widely used in various industries due to its different mechanical properties such as high hardness, good wear resistance, and high tensile strength. In the field of architecture, cold-rolled strip steel is used to make building frames, doors and windows [1]. In the automobile manufacturing, cold-rolled strip steel is used to manufacture body, door, roof, tire steel wire, spring steel strip, brake steel strip, etc. In the aerospace manufacturing, cold-rolled strip steel is used to manufacture aircraft structures, components, and bearings, shock absorption systems in engines, etc. In terms of daily necessities, cold-rolled strip steel is commonly used to manufacture stainless steel kitchenware. At the same time, it is commonly used to manufacture mobile phone battery cells, metal motor poles, etc in the field of electronic products. With the increasing demand for strip steel, the production and quality of strip steel have become increasingly important. However, due to the influence of various technical factors such as raw materials, rolling process level, and system control in the production process of strip steel, various defects often appear on the surface of the strip steel, such as white spots, scratches, holes, inclusions, scratches, iron oxide skin indentation, surface emulsification, and white lines, etc [2]. These defects have varying degrees of impact on the wear resistance, fatigue resistance, corrosion resistance, and electromagnetic characteristics of the strip steel and easily cause production accidents such as breakage, accumulation, and parking in the enterprises secondary processing. Therefore, strip steel surface detection is a very necessary and important step in strip steel production and now a large number of strip steel detection methods have been proposed.

Manual inspection is a traditional method for detecting strip steel surface defects [3], which mainly use the strobe method, but this method has low sampling rate, low accuracy, poor real-time performance, low efficiency, and is greatly influenced by manual experience. To overcome the drawbacks of the above methods, visual inspection has been widely applied. As a non-contact and non-destructive automatic detection method, it needs to build a visual inspection system, and then use image processing algorithms to identify defects in the machine vision methods [4], but the machine vision detection with a wide spectral response range is safe and reliable, can improve the detection efficiency and can work continuously in harsh environments. Now several researchers have achieved significant results in the machine vision detection of steel strips. Shu [5] added a C3 structure and NAM attention mechanism into the YOLOv5 model, which reduces the computational complexity, improves the computational speed and enhances the defects recognition ability. Shen [6] introduced the edge information into the defect detection tasks to improve the edge detection performance in multi-scale detection, resulting in a 1.6% increase in detection accuracy while improving training efficiency. Zhao [7] optimized the loss function to improve

*Corresponding Author: Xiaoning Bo; E-mail: boxn@tit.edu.cn
DOI: https://doi.org/10.70003/160792642024092505005

the detection speed, and added Coordinate Attention into the network by utilizing the lightweight and high-speed characteristics of YOLOv5 to enhance feature extraction capabilities and network multi feature recognition capability of the model. Ji [8] used the MobileViT lightweight Transformer network for detection and added an adaptive feature fusion module (ASFF) on the basis of YOLOv4. At the same time, she used K-Means++algorithm to cluster and generate prior boxes that are more suitable for position adjustment in the detection, which can reduce the missed detection rate and enhance the feature detection capability of the model.

The above network structure is mainly based on the 5th generation YOLO model, which is relatively large and cumbersome to deploy. In the actual detection, the technical level of operators is required to be high. Therefore, in order to meet the surface defects detection needs of the cold-rolled strip steel, this paper focuses on the research of the new recognition network YOLOv8 l, which has higher detection accuracy, stronger scalability and compatibility comparing with YOLOv5.

2 Surface Defects in Cold-rolled Strip Steel

In order to achieve the accurate detection of surface defects in strip steel, it is necessary to analyze the common surface defects in order to make the targeted improvements for the detection model.

- **Patches**

In the process of rolling strip steel, some production require the use of acidic emulsifiers. The residue and splashing of emulsifiers can lead to the appearance of patches defect. The patches defect on the strip steel surface are mainly irregular, and its color is bright white.

The main reason for the formation of patches is the excessive oil or chloride ions during the pickling process. The edges of the patches are irregular, but they are brighter against the surface of the steel strip. The area of the patches varies in size and shape, so bright white is its main characteristic compared with the other defects.

- **Hole**

The surface holes are mainly caused by the secondary oxidation of molten steel during the casting process of the billet, or the inclusion of slag and inclusions in the billet. They can appear as single or series plastic tensile cracks, and some may show the obvious substrate layering. The occurrence frequency of holes is relatively low, but it has a significant impact on the quality of the strip steel and can easily lead to the strip break. In the image, it can be seen that the edge shape of the hole is clear and obvious, and the grayscale of the hole is deeper than that of the strip steel image. The diameter of the hole is generally small.

- **Inclusion**

The refractory material in the heating furnace peels off on the strip steel surface, or other impurity falls off on the strip steel surface, and embedded in the surface of the strip steel after rolling.

The inclusion defect seriously affects the surface smoothness of the strip steel. If galvanized in the later stage, the quality of the coating at the defect area cannot be guaranteed. Consistent with the formation mechanism of holes, the defect of iron oxide skin indentation mainly occurs during the cold rolling process of the incoming materials. In the image, the inclusion defect generally appears as a gray black slender defect. It is irregular distribution, follows the direction of the rolling mill, and extends on the surface of the strip steel.

- **Scratches**

The formation of scratches is mainly caused by the contact between the production equipment and other hard objects on site during the processing of the strip steel. Scratches generally have a small impact on the mechanical properties of the strip steel, showing periodicity and continuity. Consistenting with the transportation and processing direction of the strip steel, the scratches depth is generally shallow, and the trajectory is generally long [9].

- **Rolled-in Scale**

Iron oxide scale indentation is an irregular surface inclusion on the surface of cold-rolled strip steel. The formation reason is that non-metallic inclusions on the surface or under the skin of the slab are broken or exposed during the strip rolling, thus forming the interlayer folding. Iron oxide scale debris indentation is a common inclusion. In the image, the gray scale of the interlayer is similar to the background, the color at the edges is darker and the size and shape are different [10].

- **Blister**

During the pickling and rolling process of carbon steel pickling plates, there are batch edge blister defects. The defect has a tongue shaped linear morphology, with a diameter of about 1 mm and a length of 10-100 mm. It is mainly distributed on both sides of the strip steel along the rolling direction. The root of the warped position is connected to the substrate, and form a long tongue shape. The grain size at the warped position is significantly larger than that of the substrate, and there is a significant decarburization phenomenon in the root tissue connected to the substrate [11].

- **Pitted Surface**

The generation of pitting is mainly due to the rough surface of the work roll after wear during the rolling process, and the oxide film on the roll surface peels off. The peeled oxide film will adhere to the surface of the cold-rolled strip steel. In the image, the pitting defects is black, manifests as the small pinhole shaped pits of varying depths, and its main features are fine, unevenly distributed.

- **Crazing**

The macroscopic morphology of crack defects is linear defects along the rolling direction. The shape of the defect is irregular and the color is black. Linear defects are accompanied by the multiple black point defects, which are the intersection or starting point of different linear defects. The length of linear defects is about 150-400 mm, and the width is 1-2mm. The size of point defects is approximately the size of a grain of rice. The overall defect is similar to a branch with many forks [12]. Specifically, the surface defect images are shown in Figure 1.

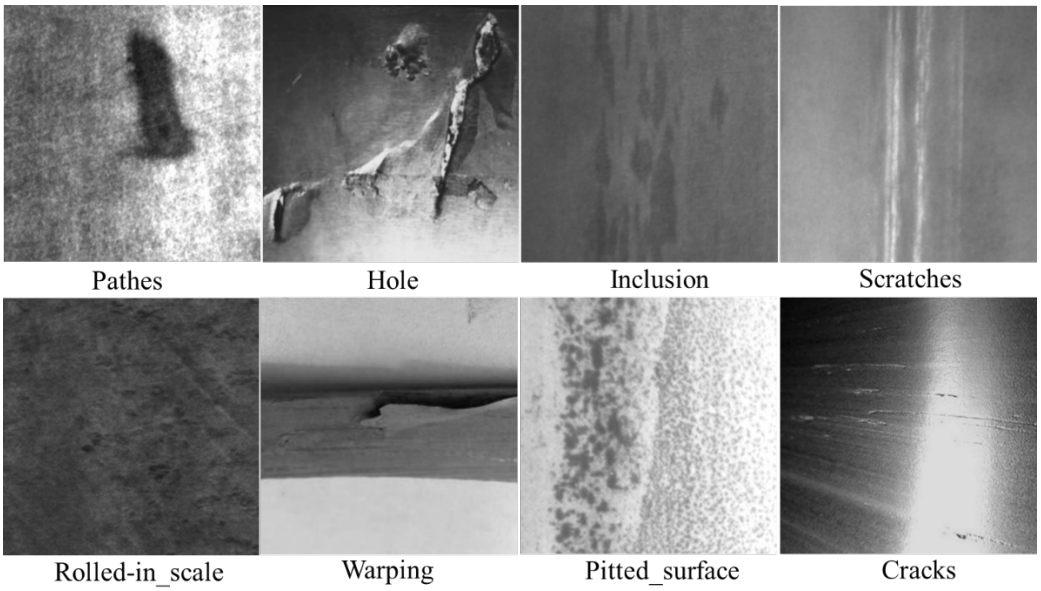

Figure 1. The surface defect images

From the above, it can be seen that the overall size of surface defects on the strip steel is relatively large, such as the paths defects. At the same time, due to the different formation mechanisms of surface defects, the size of surface defects formed in different workshops at different time periods varies. The size of the larger defects can reach several tens of centimeters, such as scratch defects, so the size of defects is diverse. In the steel actual production, each process is carried out in the strict order. Specifically, the cold-rolled steel is rolled into steel coils with large dimensions, so there is no situation where multiple defects overlap poorly generally in the cold-rolled strip steel production.

In addition, different compositions of the strip steel have different speeds during the cold rolling process. Generally, the production speed of cold-rolled strip steel is 100-1000m/s, while the rolling speed of more advanced cold rolling equipment can reach up to 1400m/s. For example, the steel enterprises that mainly produce various grades of steel such as IF steel, low alloy high-strength steel, ultra-high strength steel, and plain carbon steel, has the high-strength automotive plate acid rolling mill designed by SVAI company. The maximum force of this rolling mill is 3200 tons, and the rolling speed can reach 1400m/s, which is currently at a relatively advanced level of cold rolling [13]. Therefore, when designing the visual inspection schemes of the cold-rolled strip steel, not only detection accuracy but also the detection speed should be considered to achieve online real-time detection of the surface defects on cold-rolled strips steel.

3 Defect Detection Scheme and Image Preprocessing

As can be seen from the above, there are still the following problems in visual inspection of the strip steel surface defects:

(1) The real-time performance cannot meet the requirements. Most defect detection systems on the market can only meet the operating requirements of 1.5m/s, which does not match the current speed of steel rolling production lines.

(2) The current detection system generally only targets a single defect or the individual defects, and cannot detect all different types of defects. However, different steel companies use different equipment to produce different specifications of strip steel, and the production environments are different, so the strip steel defect are different, which produced by the different steel companies.

(3) The feature information extraction is not comprehensive, that is, the grayscale change information of defects is extracted without considering the grayscale change of the strip steel itself.

3.1 Backbone Enhanced Network

The visual detection scheme proposed in this paper is shown in Figure 2. After analyzing the cold-rolled strip steel surface defect, the input terminal and network structure of the system are improved. At the same time, in order to obtain the high-quality images, image wavelet transform is used for filtering, denoising, and Canny edge detection is applied in the image preprocessing.

3.2 Image Preprocessing

- **Image Denoising**

Due to the influence of certain interference factors in the on-site environment (such as dust and water mist), the steel strip surface detection system will be affected in the image acquisition and transmission. Therefore, it is necessary to perform denoising on the surface defect images in order to avoid affecting the subsequent detection process.

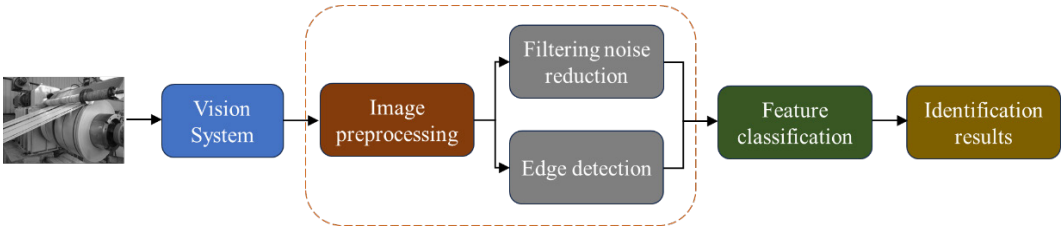

Figure 2. Defect detection scheme

In this paper, wavelet transform was used for image denoising. The main denoising principle is to rely on the inconsistency of amplitude characteristics between the image features and noise features in the wavelet domain. Wavelet transform mainly processes image in the frequency domain. Specifically, the image is firstly formed into high-frequency and low-frequency regions after wavelet transform, then denoising can be achieved by filtering different wavelet coefficients. If the wavelet coefficients in the high-frequency region with noise are lower than the set threshold, it is considered that they are mainly caused by noise, and the coefficients are set to zero. If the wavelet coefficient is higher than the set threshold, it is considered to be mainly composed of useful signals, and the coefficients are directly saved or slightly reduced. Lastly, use appropriate threshold and threshold functions to update the high-frequency coefficients in each layer, and use the new filtered coefficient to get the noise-free image. In the whole process, the selection of threshold and threshold function directly affects the image denoising, therefore, the threshold is set to be dynamically adjustable, which can maximize the retention of useful signals in this paper [14].

In detail, we set

$$\lambda_i = \frac{m|g_{ik}|}{\Delta\omega} \bullet \sqrt{2\ln N_i} / e^{\frac{i-1}{2}}. \quad (1)$$

Where λ_i represents the threshold of the i-th layer in the wavelet decomposition, $\frac{m|d_{ik}|}{\Delta\omega}$ represents the noise variance of high-frequency coefficients in each layer of wavelet decomposition. N_i represents the total number of wavelet coefficients in each layer. Obviously, this threshold is adaptive, it will decay as the number of layers increases, and can ensure each layer to utilize its own noise variance and wavelet coefficient.

At the same time, the threshold function is improving, and the threshold function is as follows:

$$\widehat{A_{ij}} = \begin{cases} \Delta\omega - \frac{\lambda_i}{1.57} \bullet \arctan\left(\frac{\lambda_i}{1.57} * \Delta\omega\right), |\Delta\omega| \geq \lambda_i \\ 0.01 * \Delta\omega, |\Delta\omega| < \lambda_i \end{cases}. \quad (2)$$

The curve of the improved threshold function is shown in Figure 3.

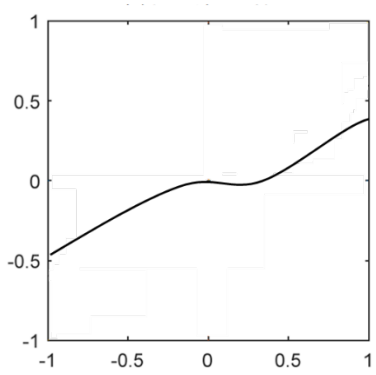

Figure 3. The curve of the improved threshold function

The image denoising result are shown in Figure 4.

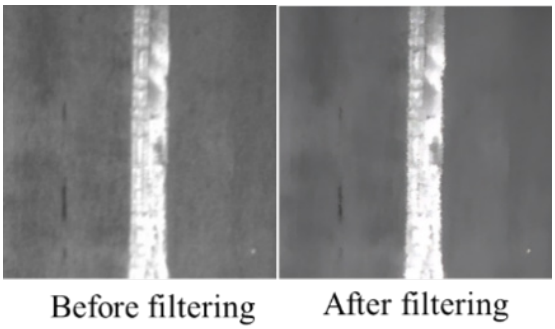

Figure 4. The image denoising result

- **Image Edge Detection**

Considering the characteristics of high noise and large scale variation in defect samples of cold-rolled strip steel, the Canny algorithm is improved in this paper [15]. The specific details are as follows.

1) Replace Gaussian filtering in classical Canny algorithm with wavelet denoising, and perform adaptive threshold smoothing to reduce feature false detection rate.
2) Calculate the pixels gradient amplitude and direction information in the image, and obtain the edge strength and direction of each pixel point.
3) Non maximum suppression is applied for the gradient amplitude on the basis of obtaining gradient direction information, in order to obtain the segmentation result of edge detection further. Then the gradient is divided into 8 uniform regions according to the plane coordinate direction.

4) Use the Otsu algorithm to calculate the segmentation threshold, so that the threshold can be automatically adjusted based on high and low frequency regions.

The edge detection result is shown in Figure 5.

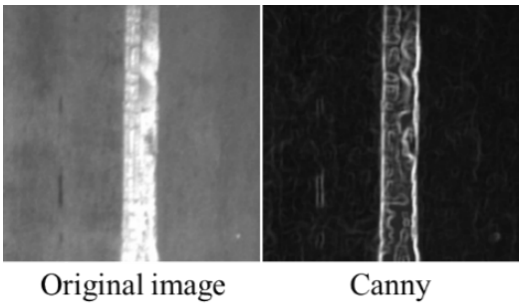

Figure 5. The image edge detection result

4 The Improved YOLOv8 Model

In the fast cold-rolled strip steel production, the surface defect size is large, no overlap and there are many types. In order to accurately detect defects in this situation, the latest YOLOv8 as the basic detection algorithm is used r, which mainlyYOLOv8 is improved in this paper， The YOLOv8 model, released by Ultralytics in January 2023, is currently the most advanced detection model of the YOLO series. Compared to YOLOv5, YOLOv8 introduces a new backbone network, a new anchor free detection head, and a new loss function. Therefore, the YOLOv8 model is easier to train and adjust, has faster inference speed and higher accuracy, and has broad application prospects in defect detection. In this paper, there are three improvements for the YOLOV8 model: the addition of attention module CA [16], the improvement of convolution kernel, and the replacement of loss function.

4.1 The Addition of CA Attention Mechanism

The model structure of CA attention mechanism is shown in Figure 6. The CA attention mechanism integrates the positional information of feature maps into the channel attention, allowing for the simultaneous consideration of both the channel dimensions features and the spatial dimensions features. Therefore, the mechanism increases the coverage range of feature information with adding a small amount of computational complexity.

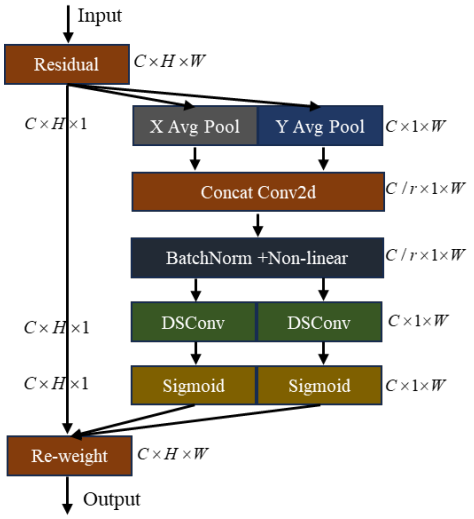

Figure 6. The model structure of CA attention mechanism

In the first stage of the CA module, perform horizontal and vertical average pooling operations on the input feature map, and obtain the feature maps $z_c^h(h)$ and $z_c^w(w)$ (C represents the channel), then aggregat the features in two directions to help accurately locate the target area for defect detection. In the second stage, the coordinate attention is generated. Transform the two feature maps generated in the previous cascade using the below function:

$$y = S\left(T_1\left(z^h, z^w\right)\right). \tag{3}$$

where S is a nonlinear activation function, $[z^h, z^w]$ represents the connection operation along the spatial dimension, y is the intermediate feature mapping for encoding the target feature space information in both horizontal and vertical directions. Specifically, the position of CA in the YOLOv8 model is shown in Figure 7.

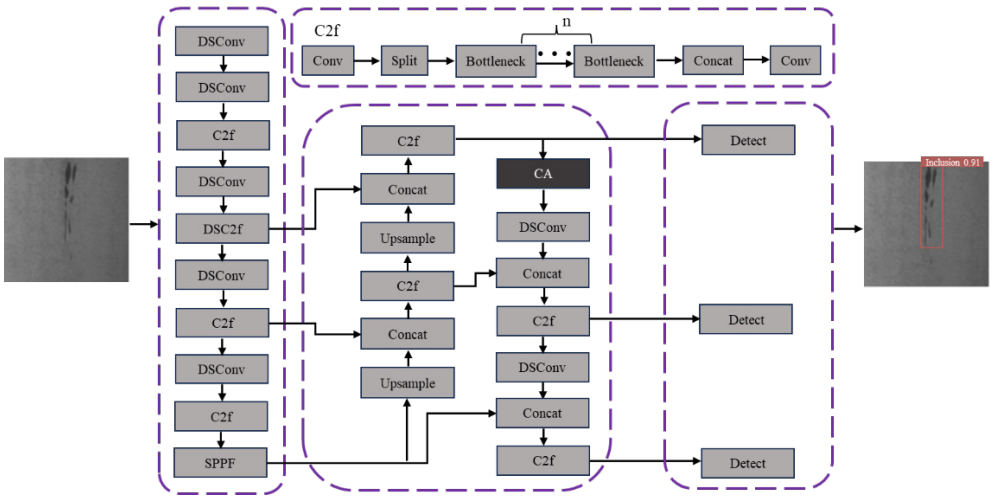

Figure 7. The position of CA in the YOLOv8 model

4.2 The Lightweight Processing of YOLOv8

To achieve the lightweighting of YOLOv8, a lightweight depthwise separable convolution model DSC (Depthwise) [17], which can significantly reduce the number of network parameters compared to the regular convolution, is used to replace the traditional convolution module in the model Neck section. The deep separable convolution consists of the channel wise convolution (DW) and the point wise convolution (PW). DW convolves the pixels on each channel to obtain their respective features. The size of the convolution kernel is 3×3, and the number of convolution kernels is equal to the number of input channels. PW adopts a convolution kernel of size 1×1 to convolve features on different channels at each pixel. The DSC is shown in Figure 8.

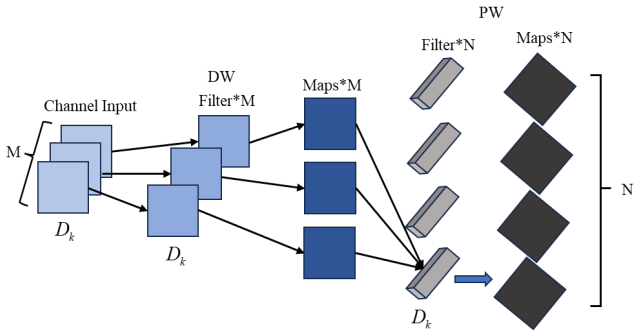

Figure 8. The depth wise separable convolution DSC

Assuming the input feature map has a length of H, a width of W, M input channels, N output channels, and the convolution kernel size of $H_K \times H_K$, the computational cost of the depthwise separable convolution is:

$$T = H \times W \times M \times N + H \times W \times M \times H_K \times H_K . \quad (4)$$

Obviously, the computational complexity is reduced to $\left(\frac{1}{N}+\frac{1}{D_k^2}\right)$ times of the original standard convolution computational complexity after using the DSC, the computational complexity and model parameters have been reduced, thereby achieving the model lightweight processing and improving the detection speed.

4.3 The Lightweight Processing of YOLOv8

The detection performance of the system is closely related to the design of the regression loss function, and the improvement of the loss function can help to enhance the ability of object detection. In the original YOLOv8 model, the loss function is CIoU. But considering the issues such as sample balance, the WIoU [18] function is used to replace the loss function CIoU, in order to improve the model convergence speed and reduce false detection rate.

The loss function are as follows:

$$S_{Loss} = S_{AFLoss} \cdot L_{IoU} . \quad (5)$$

$$S_{AFLoss} = \exp\frac{\left(x_{AF} - x_{tar}\right)^2 + \left(y_{AF} - y_{tar}\right)^2}{W_{\min}^2 + H_{\min}^2} . \quad (6)$$

where S_{Loss} represents the loss of high-quality anchor frames, (x_{AF} , Y_{AF}) represents the position of the anchor box corresponding to the position of the target box (x_{tar}, Y_{tar}), ($W_{\min}$, $H_{\min}$) represents the height and width of the minimum anchor box respectively. This method does not define the overlapping area and aspect ratio in the loss, eliminate the impact of sample imbalance and thus improve the convergence speed of the model.

In addition, the focusing coefficient δ_{Loss}^* is utilized to make the model more focused on the difficult samples and improve the detection performance. Here,

$$S_{Loss}^{'} = \delta_{Loss}^* \cdot S_{Loss} . \quad (7)$$

In the model training process, δ_{Loss}^* decreases as the loss of IoU decreases.

5 Experiment

5.1 Experimental Dataset

In this paper, experiments were conducted by using the NEU-DET dataset of surface defects on steel strips which are publicly available at Northeastern University. The dataset contains six types of defect images: rolled-in scale (RS), crazing (Cr), pitted surface (PS), patches (Pa), scratches (Sc), inclusions (In). Add the dataset of hole and crack images into the NEU-DET dataset, and obtain an experimental dataset containing 2400 images, in which each defect has 300 images. In order to enhance the stability of the defect detection model, add an additional 4800 images into the dateset by cropping, rotating, and other methods. The dataset is split in a 7:1:2 ratio, that is, the training set contains 5040 images, the validation set contains 720 images, and the test set contains 1440 images.

5.2 Experimental Environment

The experimental environment settings are shown in Table 1.

Table 1. The experimental environment

Name	Parameter
System environment	Ubuntu 22.04
Processor	Intel core i7 14650HX
Graphics card	NVIDIA RTX4060,8GB
Memory	32GB
Programming environment	Python 3.8, PyTorch 1.11.0 framework
Resolution	640*640
Iterations	120

5.3 Evaluating Indicator

In this experiment, the evaluation indicators are the recall (R), the accuracy (P), and the average precision (mAP), respectively. The representation of each evaluation indicator are as follows:

$$P = \frac{T_P}{T_P + F_P} . \quad (8)$$

$$R = \frac{T_P}{T_P + F_N} . \quad (9)$$

$$mAP = \sum P / N . \quad (10)$$

5.4 Experimental Results

In order to demonstrate the effectiveness of the improved model proposed in this paper, the ablation experiments, the comparative experiments with other models, and the image detection experiments are conducted.

- **The Ablation Experiments**

The ablation experiment was conducted by combining multiple modules, and the experimental results are shown in Table 2. Obviously, In the case of only integrating the attention module CA, mAP significantly improved by 1.8%, but the change in recall is small, and the detection speed decreased by 1.32%. After replacing the convolutional kernel to achieve the lightweight network, the recall and the detection speed of the model have significantly been improved by over 1.5%, but the accuracy has slightly decreased, with a decrease of no more than 0.8%. After improving the loss function, the overall detection performance of the model such as the recall, the accuracy, and the average precision has significantly improved.

Table 2. The ablation experiments result

Models	R (%)	P (%)	mAP	FPS
YOLOv8	75.7	83.2	83.1	213
YOLOv8+CA	75.7	83.3	84.9%	210
YOLOV8+CA+DSC	77.3%	82.4%	85.3%	226
YOLOV8+CA+DSC+WIoU	77.9%	86.4%	86.3%	237

- **The Comparative Experiments**

Comparing the improved model proposed in this paper with the current classic detection models: SSD, YOLOv5, and YOLOv8 prototypes, in order to verify the performance of the proposed model. The results are shown in Table 3.

Table 3. The comparative experiments result

Models	R (%)	P (%)	mAP	FPS
SSD	63.8	73.7	69.9	56.3
YOLOv5	68.9	77.9	73.6	167
YOLOV8	75.7	83.2	83.1	213
YOLOV8Improvement	77.9%	86.4%	86.3%	237

- **The Image Detection Experiments**

In order to demonstrate the improvement of model performance, the patches defect and rolled in scale defect in actual scenarios were applied in this experiments, and the detection effects of the model before and after improvement was compared. The comparison effect is shown in Figure 9, the left side shows the detection results of the original YOLOv8 model, while the right side shows the detection performance of the improved model. It can be seen that the improved model significantly improves the detection results for the patches defect.

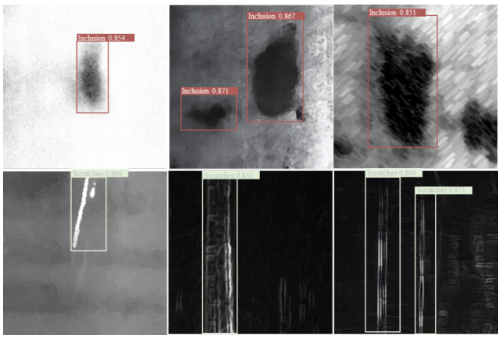

Figure 9. The comparison effect

6 Conclusion

In order to solve the problems of low detection accuracy, easy occurrence of false detection, missed detection, and long time consumption in the current cold-rolled strip steel surface defect detection model, this paper proposes an improved cold-rolled strip steel detection YOLOv8s model. Firstly, add the CA attention mechanism into the model to improve the accuracy of defect detection. Then improve the original convolution kernel to enhance the convergence speed of the model and reduce the volume of the model. Finally, the loss function is improved to enhance the detection accuracy. The proposed model was validated on the NEU-DET dataset, and the experimental results showed that the proposed method effectively improve the detection efficiency of the cold-rolled strip steel surface defects.

Acknowledgement

This work is supported by Scientific and Technological Innovation Programs of Higher Education Institutions in Shanxi (2022L534, 2022L533)

References

[1] Y. Liu, *Research and Application of Online Detection Algorithm for Surface Defects of Cold Rolled Strip Steel*, Ph. D. Thesis, University of Science and Technology Beijing, Beijing, China, 2020.

[2] L.-J. Shi, *Research on Algorithm of Strip Surface Defect Identification Based on Machine Vision*, Master's Thesis, Taiyuan University of Technology, Taiyuan, China, 2022.

[3] K. Xu, P. Zhou, C.-L. Yang, On-line Detection Technique of Tiny Surface Defects for Metal Plates and Strips Based on Photometric Stereo, *Journal of Mechanical Engineering*, Vol. 49, No. 4, pp. 25-29, February, 2013.

[4] Y.-Y. Liu, *Similar Defect Recognition of Cold Rolled Rust-free Strip Surface Based on Binocular Stereo*

Vision, Master's Thesis, Taiyuan University of Technology, Taiyuan, China, 2020.
[5] R. Shu, Steel surface defect detection based on improved YOLOv5s algorithm, *Agricultural Equipment & Vehicle Engineering*, Vol. 61, No. 12, pp. 148-151+160, December, 2023.
[6] K.-Y. Shen, X.-F. Zhou, X.-B. Fei, Y.-Z. Chen, J.-Y. Zhang, C.-G. Yan, Boundary-Aware Deeply Residual Network for Salient Object Detection of Strip Steel Surface Defects, *Journal of Applied Sciences*, Vol. 41, No. 6, pp. 978-988, November, 2023.
[7] X.-T. Zhao, Y.-H. Liu, Surface defect detection of strip steel based on improved YOLOv5, *Automation & Instrumentation*, No. 10, pp. 6-9, October, 2023.
[8] J.-J. Ji, J. Wang, Y.-J. Chen, D.-H. Lu, Surface defect detection of hot rolled strip based on improved YOLOv4, *Computer Engineering and Design*, Vol. 44, No. 9, pp. 2786-2793, September, 2023.
[9] L. Kang, Analysis and Control of Surface Defects in Cold Rolled Strip Steel, *Shanxi Metallurgy*, No. 12, pp. 266-268, September, 2023.
[10] J. Xiao, Discussion on removal and collection method of iron oxide scales in finishing process, *Steel Rolling*, Vol. 37, No. 5, pp. 44-46, October, 2020.
[11] S.-Q. Wang, L.-M. Jiang, C.-C. Han, D. Cheng, D. Zhou, Cause analysis and control of surface warping defect of low carbon cold rolled strip, *Hebei Metallurgy*, No. 1, pp. 59-63, January, 2022.
[12] J. Zou, *Study on Longitudinal cracks of SPHC Hot Rolling Strip in CSP Plant*, Master's Thesis, Wuhan University of Science and Technology, Wuhan, China, 2014.
[13] H.-T. Wang, R. Su, Q. Wang, T. Gu, J. Zhao, Y.-G. Yu, Study on the Formation Mechanism of Emulsion Stains on the Surface of Cold-rolled Strip Steel, *Shanxi Metallurgy*, No. 1, pp. 84-85+98, January, 2023.
[14] Y.-B. Hu, X. Zhou, A.-G. Shen, Y. Hu, Image denoising and fusion based on improved wavelet transform, *Journal of Qiqihar University(Natural Science Edition)*, Vol. 39, No. 3, pp. 33-38, May, 2023.
[15] Z.-H. Liu, *Implementation and Application of an Improved Canny Algorithm for Image Edge Detection Based on FPGA*, Master's Thesis, Yancheng Institute Of Technology, Yancheng, China, 2023.
[16] Y. Li, *Classification of Plant Disease Based on Improved CondenseNetV2 and Adversarial Attack*, Master's Thesis, Guilin university of technology, Guilin, China, 2023.
[17] J.-J. Hu, *Study of Pneumonia Medical Image Classification Based on Depthwise Separable Convolutional Neural Network*, Master's Thesis, Dalian Maritime University, Dalian, China, 2023.
[18] H.-W. Chai, *Research on detection and tracking of humans and vehicles*, Master's Thesis, Huazhong University of Science & Technology, Wuhan, China, 2020.

Biographies

Xiaoning Bo received the M.S. degree in Beijing Jiaotong University. He is currently a PhD student in North University of China and working as an lecturer in Taiyuan Institute of Technology. His current research fields include computational imaging and image processing.

Jin Wang received the M.S. degree in Communication Engineering from Yanshan University. She is currently working as an associate professor in Taiyuan Institute of Technology. Her current research fields include image processing and computer vision.

Yongqiang Zhao received the M.S. degree in Taiyuan University of Technology. He is currently working as an professor in Taiyuan Institute of Technology. His current research fields include image processing, signal detection and processing.